

4.3.1 COMPARISON OF MEDIUM FREQUENCY PULSED RADAR INTERFEROMETER AND  
CORRELATION ANALYSIS WINDS. 1.

C. E. Meek, I. M. Reid, and A. H. Manson

Institute of Space and Atmospheric Studies  
University of Saskatchewan  
Saskatoon, Canada S7N0W0

18939

SC 683460

## INTRODUCTION

In principle, the interferometer analysis determines the radial velocity and direction of single scatterers provided that each has a sufficiently different Doppler frequency to permit separation by spectral analysis. In fact, scatterers will not have constant radial velocity, and their Doppler frequencies as well as their directions will be modulated by their horizontal motion. Thus, there is a tradeoff between the poorer resolution but less "smeared" scatterers on shorter records and the higher resolution (longer) records.

Three or more non-collinear scatterers are sufficient to determine the wind.

## EXPERIMENTAL APPARATUS

Figure 1 shows the antenna arrays used, N-S linear is transmitted and E-W linear is received. The recording system, designed by D. G. Stephenson (GREGORY and STEPHENSON, 1972), records raw (8 bit) data simultaneously for 2 channels at 24 height gates and sends it directly to an incremental tape drive. This permits a maximum transmitter pulse rate of 15 Hz, which gives a final sample separation at each antenna of 0.2 sec. At this rate, there is one pulse dropped every 12 sec (8640 bytes) while a block gap is written on tape. Data can be recorded for up to 8 hr (1 tape) in this fashion.

The in-phase (I) and quadrature (Q) outputs of the coherent receiver are 5° in error; this will result in a weak (~-27dB) sidelobe at the negative Doppler frequency of any signal and is not expected to affect the present results.

## ANALYSIS

The data to be discussed consist of 3.6-min lengths starting every 5 min. The I and Q amplitude sequences for each antenna are first tapered along 10% of their length at each end by a cosine function to reduce sidelobes, and then Fourier transformed (1024 points). The cross spectra (which are not smoothed) for pairs of antennas yield the phase differences,  $\Delta\phi$ , to be used in angle of arrival. These are corrected for cycling delays caused by the recording technique of sampling each antenna in rotation. Since there are only 3 receiving antennas, there is no over-determination of phase, and the only basis left for selecting single scatterers is by peaks in the power spectra. The criteria for selecting Doppler frequencies are: that all antennas should show a local peak in the power spectrum, and that the average (dB) power of the selected peak should be at least 5 dB greater than the average power near the Nyquist frequency, and within 30 dB of the power of the strongest selected peak.

The phase differences at the selected frequencies are then corrected for unequal antenna cable lengths, and an attempt to correct for phase folding is done. Phase folding occurs beyond a real zenith angle of about 30° (depending on azimuth) due to the 1-lambda spacing of the receiver array, and must be

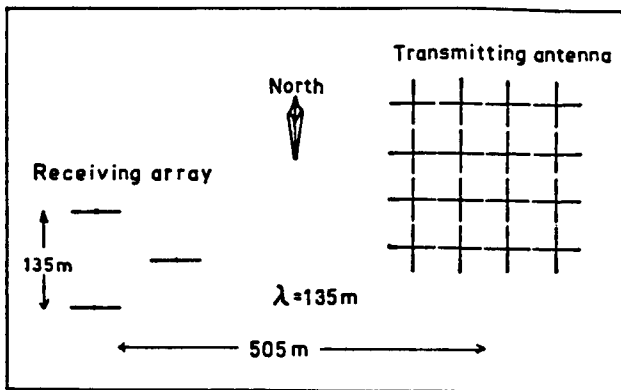


Figure 1. Receiving and transmitting arrays.

considered because of the transmitter antenna sidelobes at  $45^\circ$ ; it will affect both the calculated zenith and azimuth angles. The correction procedure is to check whether the three  $\Delta\phi$  add to zero -- if they do not, then the  $\Delta\phi$  with the maximum absolute value is modified by  $360^\circ$ ; if the resulting sum is still non-zero, the peak is rejected. This method is not foolproof, since scattering at very large zenith angles can fold two of the  $\Delta\phi$  and look immediately acceptable. The only real solution is closer antenna spacing, and the use of loop antennas to reduce the subsequent increase in coupling.

#### DATA

A sample record is shown in Figure 2. The left side shows power spectra for the three antennas and selected peaks are marked at the bottom (originally 3 colours). The right side plots the direction (zenith angle is log scale with origin = 1) and the horizontal component of velocity calculated on the assumption that the real vertical component is negligible. Figure 3 shows relative power versus zenith angle. The number of cases are printed on the plot. Also shown is the theoretical transmitter beam pattern (one way) for the N-S plane. Phase folding is probably responsible for the partial filling of the theoretical null in this pattern; little difference was seen when the azimuths were divided into two parts, one looking towards the sidelobes and the other between them.

#### FULL CORRELATION ANALYSIS

Data were averaged in threes (giving  $t = 0.6$  sec) before performing lagged complex correlations. The magnitudes of the correlations were used to calculate apparent (from just the time lags of the peak correlation) and true (using, in addition, the width of the mean auto and the magnitudes of the peak cross correlations) velocities. The mean vertical velocity is found from the slope of the autocorrelation phase near zero lag. The correlations for the data used in Figure 2 are shown in Figure 4.

#### VELOCITY FROM INDIVIDUAL "SCATTERERS"

This is found by a least squares fit of a 3-D or 2-D (horizontal) velocity vector to the data, which minimizes the squared error in radial velocity. The squared error is first weighted by the power of the Doppler peak relative to that of the largest peak power in each record. In practice, the resulting

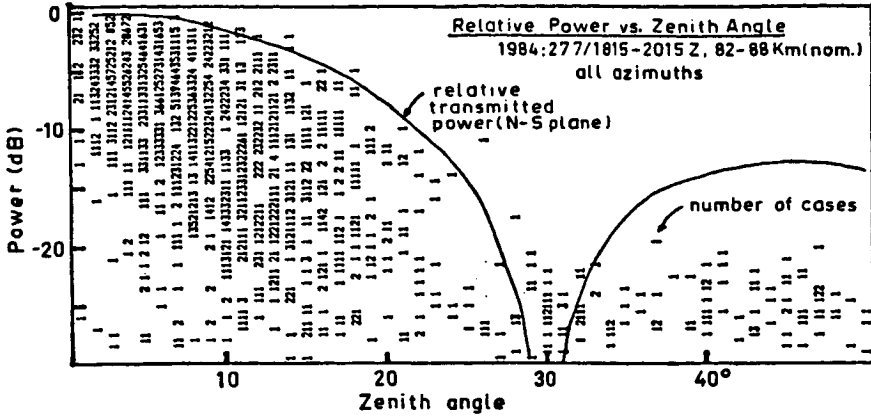


Figure 2. Power (relative to the maximum selected peak in each record) versus calculated zenith angle for a 2 hr period (24 records).

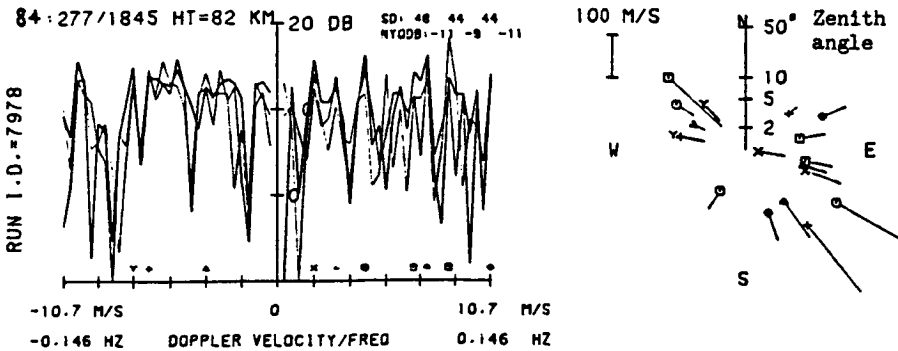


Figure 3. Spectra for 3 antennas shown over a small frequency range (full range is + 2.5 Hz); symbols indicate chosen peaks and appear on the scatterer location plot at the right as well, where inferred horizontal velocity is shown as a straight line emanating from the scatterer symbol.

vector was found to be relatively independent of the actual weighting used. A lower zenith limit of 5° was used to reduce error due to inaccurate cable length corrections, and an upper limit of 15 to avoid cases of phase folding (a zenith angle of 50° can fold back to 22°). In addition, an upper limit of 40 m/s was placed on the radial velocity -- this also acts as a power limit, since spectra peak near zero frequency.

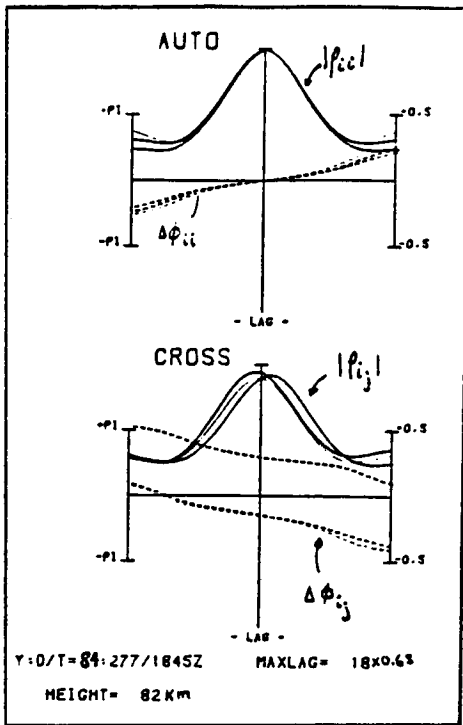


Figure 4. Auto and cross correlations for the record shown in Figure 3.

#### VELOCITY COMPARISON

Table 1 lists the velocities for the record shown in Figures 2 and 4.

TABLE 1

Comparison of velocities for 1 record (82 km, 1984: 277/1845Z).

	speed (m/s)	direction (E of N)	vertical (m/s)
interferometer analysis (12 Doppler peaks)			
3-D	58	132	1.6
2-D	56	123	
correlation analysis			
apparent	45	123	0.4
true	32	145	

The mean velocities for 1 hour of data (12 records) are shown in Figure 5; most records have correlation  $V_z$  values, fewer have apparent, and fewer still, true velocities. The interferometer value was found by one fit to all the individual scatterers found in the hour. Because the height variation for constant range over  $5^\circ$ - $15^\circ$  zenith is within the height resolution of the system

(3 km), no adjustment was made to get real height. Also shown are the mean values (9 km resolution) from the real-time analysis (non-coherent) system.

## DISCUSSION

Figure 5 shows that the "apparent" speed agrees with the interferometer value, but the "true" velocity is about half the latter. If it can be shown that the chosen Doppler peaks represent actual single localized scattering regions, then the "true" velocity is in error. This cannot be shown with just one record, because a peak in the spectra can be translated either as a single scatterer, where the  $\Delta\phi$  represent the angle of arrival and the Doppler frequency defines the radial velocity, or alternately as a Fourier component of a rigid pattern, where the  $\Delta\phi$  represent the wavelength and propagation direction, and the Doppler frequency is related to the phase speed of the "wave". The latter concept gives the "2-D" velocity mentioned previously if it is assumed that the "wave" is a frozen-in component of a rigid pattern - viz. its calculated velocity is only a component of (and thus, in general, smaller than) the real horizontal velocity.

In theory, the use of a larger receiving array does not help to resolve this ambiguity; however, it does increase the degrees of freedom used in the peak selection (effectively a coherence criterion).

Another situation in which peaks may be mistaken for single scatterers is when signals due to several real scatterers overlap in the same frequency bin, either simultaneously or sequentially in one record. Figure 6 shows contours of constant Doppler frequency in space, assuming a constant horizontal velocity. Scatterers positioned anywhere on one contour will have the same radial velocity/Doppler frequency and their radial velocity varies linearly with time. (The plot has assumed constant range; constant height, which is more realistic, bends the contours near the ends -- about 5% change in  $\lambda$  at 15° zenith.)

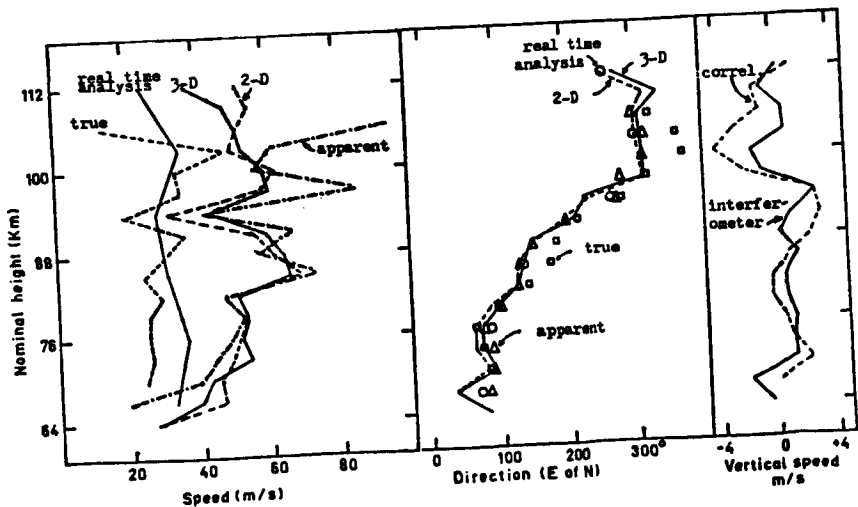


Figure 5. Comparison of interferometer and correlation analysis (apparent and true) horizontal speed and direction and vertical speed over one hour (84:277/1815-2015 GMT). Also shown are the mean winds for the real-time wind system.

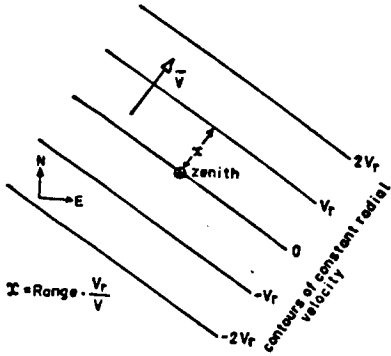


Figure 6. Contours of constant radial velocity as a function of horizontal distance from the zenith.

A simple numerical model shows that the sum of signals due to any set of scatterers (random phase and constant radial velocity over the "record length") placed along one of these contours results in a calculated scatterer located somewhere on the same contour; so there should be no bias in the resulting velocity due to lack of frequency resolution. Also, the composite scatterer, if tracked, moves with the same velocity.

Cases where two or more scatterers "scan" across one frequency bin at different times during a record are more difficult to analyze. Some local Doppler peaks will result just because the spectrum is not smooth. A more complicated model is required to see the effects. It appears that the positions of calculated scatterers would be unrelated to those of the real ones.

Finally, it is interesting to note that the vertical velocities shown in Figure 5 from the correlation method seem to have a smoother height profile than those from the individual Doppler peaks. Correlation techniques are more computationally efficient, and may even produce a more satisfactory value of  $V_z$ .

#### CONCLUSION

From these limited experimental data, it appears that the velocity found from the combined interferometer peaks agrees well with the "apparent velocity" from correlation methods, but the "true velocity" is a factor of 2 smaller. This difference might be resolved by searching for "scatterers" showing regular movement between adjacent records, and this is the subject of the accompanying paper.

#### REFERENCE

Gregory, J. B., and D. G. Stephenson (1972), High altitude winds from radio reflections, Canadian Research and Development, March/April.